PHYSICAL REVIEW B VOLUME 35, NUMBER 18 15 JUNE 1987-II

Rapid Communications

The Rapid Communications section is intended for the accelerated publication of important new results. Since manuscripts submitted to this section are given priority treatment both in the editorial office and in production, authors should explain in their submittal letter why the work justifies this special handling. A Rapid Communication should be no longer than 3½ printed pages and must be accompanied by an abstract. Page proofs are sent to authors, but, because of the accelerated schedule, publication is not delayed for receipt of corrections unless requested by the author or noted by the editor.

X-ray photoelectron diffraction at high angular resolution

J. Osterwalder, E. A. Stewart, D. Cyr, and C. S. Fadley
Department of Chemistry, University of Hawaii, Honolulu, Hawaii 96822

J. Mustre de Leon and J. J. Rehr
Department of Physics, University of Washington, Seattle, Washington 98195
(Received 9 February 1987)

We present x-ray photoelectron diffraction (XPD) measurements at an angular resolution of $\sim \pm 1.0°$ which is much higher than in any prior study. Emission from the Ni $2p_{3/2}$ core level of Ni(001) under Al $K\alpha$ excitation is considered. The azimuthal XPD patterns are found to exhibit considerable fine structure not observed previously, including peaks whose full widths at half-maximum intensity are only a few degrees. The experimental data are found to be well described by single-scattering-cluster calculations with spherical-wave scattering. Fine structure due to Bragg-like scattering (Kikuchi bands) is also observed in both experiment and theory.

X-ray photoelectron diffraction (XPD) is by now being used in several ways for determining surface atomic structure.[1-7] Measurements can be performed in two modes so as to produce photoelectron interference effects that provide information about atomic positions: by scanning electron emission direction above a surface,[1,2,4,5,7] which requires a rotatable sample manipulator, and by scanning photon energy,[3] which requires tunable synchrotron radiation. At higher energies of $E_{\rm kin} \gtrsim 500$ eV, strong forward scattering of the photoelectron wave by nearest-neighbor atoms along bond directions can in some cases, such as molecular adsorbates and epitaxial systems, be directly related to pronounced peaks in a polar or azimuthal scan.[2,5,6] A straightforward single-scattering-cluster (SSC) model has also proven adequate for describing such data in more detail.[1,4,6]

In this Rapid Communication we report on the significant additional fine structure that can be observed in XPD at high angular resolutions of $\sim \pm 1.0°$. We also discuss to what extent the SSC model[4] is able to describe these very rich XPD patterns, and consider the degree to which Bragg-like scattering related to Kikuchi bands is observable in both experiment and theory. A clean Ni(001) surface has been chosen for study since its structure is well known and stable.[8] Also, as a test of the applicability of an SSC description to XPD, such multilayer photoemission from a thick, semi-infinite substrate represents a worse case as compared to adsorbate or thin-overlayer emission, because the presence of rows of atoms along or near the emission direction makes various types of multiple-scattering events more likely to occur.[1,4,9,10]

The experiments were performed on a Vacuum Generators ESCALAB5 spectrometer equipped with a custom-built specimen manipulator that permits a two-axis sample rotation with a precision of $\pm 0.2°$.[4] Al $K\alpha$ radiation was used for excitation. The angular acceptance cone was precisely limited for all emission points on the surface to within $\pm 1.5°$, using a stainless-steel tube array placed between specimen and transfer lens, as discussed in detail elsewhere.[11] According to model calculations, the *average* deflection angle through this array is only about $\pm 0.7°$.[11] The high-symmetry directions of the Ni crystal were located to within $\pm 0.3°$, using strong low-index XPD peaks,[1,4] and the (001) surface was periodically cleaned using standard procedures. Contaminant levels were negligible (typically 5%–10% of a monolayer).

As an illustration of the effects of higher resolution, Fig. 1 compares Ni $2p_{3/2}$ azimuthal scans for Ni(001) at $\theta = 47°$ (see inset in Fig. 1) obtained with a single $\pm 3.0°$ aperture and with the $\pm 1.5°$ tube array. The crystal was not moved in θ between the two scans, and only the ϕ scale was reset. The data for the tube array show a dramatic increase in fine structure, thus demonstrating how quickly angular averaging can distort such diffraction patterns. Some of the finer features have a width of only a few degrees, such as the symmetry-related peaks d at $\phi = 21°$ and 69°.

In Fig. 2(a) we show a portion of the large and detailed data set obtained for Ni(001), in particular the intensity variations over the solid-angle range $40° \leq \theta \leq 50°$ and $0° \leq \phi \leq 90°$. This intensity surface is derived from eleven separate azimuthal (ϕ) scans, each being taken

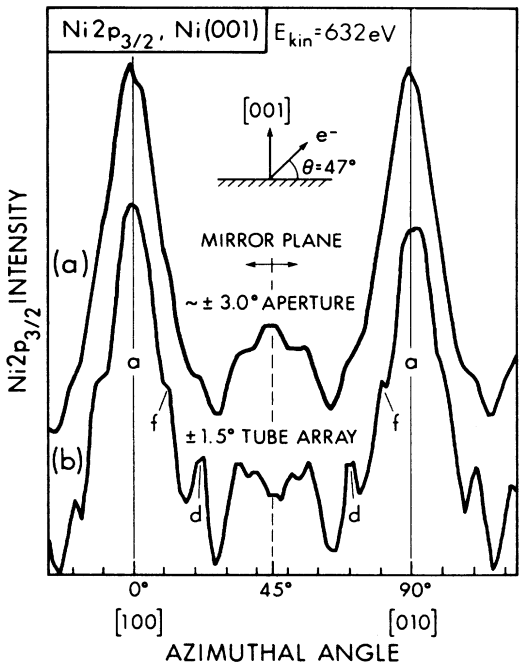

FIG. 1. The effect of improved angular resolution on XPD patterns of Al $K\alpha$-excited Ni $2p_{3/2}$ emission from Ni(001). Azimuthal scans at $\theta=47°$ are shown for (a) $a \pm 3.0°$ single aperture and (b) $a \pm 1.5°$ tube array.

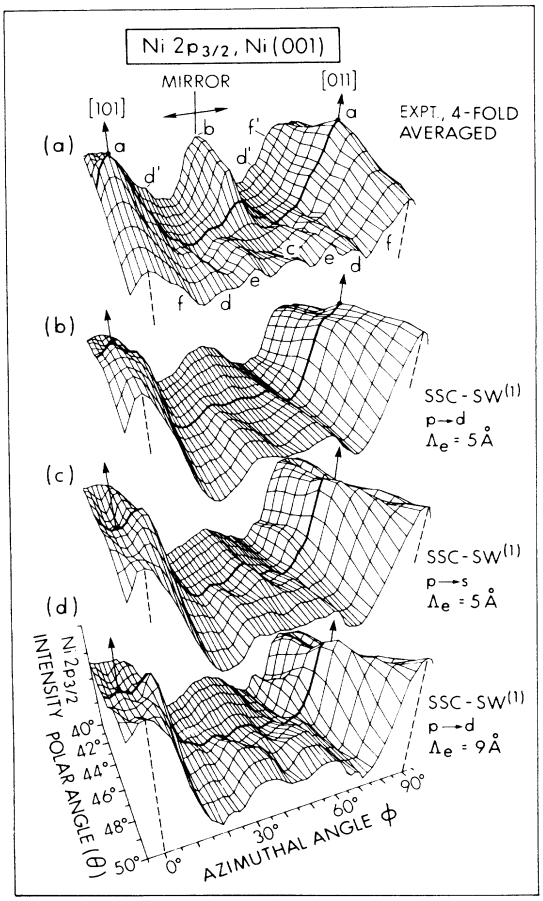

FIG. 2. Summary of a closely spaced series of high-resolution Ni $2p_{3/2}$ azimuthal scans from Ni(001). The experimental data are shown in (a), after being fourfold averaged from a full 360° scan. However, all features seen here were seen as well in each individual quadrant. In (b), SSC-SW[(1)] calculations assuming the dominant d-wave final state and $\Lambda_e=5$ Å are shown, whereas in (c) calculations for an s-wave final state and $\Lambda_e=5$ Å are shown separately. (d) illustrates the effect of decreased inelastic attenuation with $\Lambda_e=9$ Å on the d-channel results of (b).

over 360° in 1.8° steps and fourfold averaged over symmetry-related angles into one quadrant. The polar angle θ was incremented by only 1.0° between two consecutive ϕ scans. In making this three-dimensional plot, a polar scan along $\phi=0°$ and a polar scan from a polycrystalline sample were used to properly normalize the individual ϕ scans to one another, thus eliminating rather precisely the purely instrumental variation of intensity with θ.[4]

Figure 2(a) makes it clear that XPD features can change extremely rapidly with either θ or ϕ. (Note that the θ scale is highly expanded relative to the ϕ scale.) The maximum anisotropy $(I_{max}-I_{min})/I_{max}$ in this data occurs at $\theta=45°$ and is a very high 57%. The low-index direction [101], and its symmetry equivalent [011], are both included in the data, and they point from a typical emitter toward nearest-neighbor Ni atoms. These directions coincide with strong forward-scattering peaks (features a) with a full width at half-maximum (FWHM) intensity above adjacent minima of 24° in ϕ and about 18° in θ. (The latter value was obtained from a polar scan at $\phi=0°$ over a much larger θ range.)

Additional simple forward-scattering features along other nearest-neighbor directions may be present in Fig. 2(a). The [111] direction associated with more-distant-neighbor scattering corresponds to $\theta=35.3°$ and $\phi=45.0°$, which is about 5° in θ off the data of Fig. 2(a); however, it appears that the forward-scattering peak due to this direction is rising already at $\theta=40.0°$, $\phi=45.0°$ (feature b). The [112] direction is located at $\theta=54.7°$, $\phi=45.0°$, and a peak due to this may be suggested by the small peak at the bottom of Fig. 2(a) (feature c). Although feature c is rather weak, an additional azimuthal scan at $\theta=54.7°$ indeed shows a very pronounced peak centered at $\phi=45.0°$. However, it has been pointed out in a prior analysis of epitaxial XPD that emission along such higher-index directions may involve more complex superpositions of several scattering events.[6] In addition, there are other features like the four smaller ridges at $\phi\approx 22°$, 35°, 55°, and 68° (features d,e) and some weaker shoulders (features d',f,f') whose origins are not as simple to attribute to specific scattering events.

In order to more quantitatively understand this data, we have carried out SSC calculations over the same solid angle as the data presented. The general formalism used in this model has been described by Kono, Goldberg, Hall, and Fadley.[1] However, we have gone beyond earlier cal-

culations in that spherical-wave scattering effects have been incorporated by using an effective complex scattering factor as discussed by both Rehr and co-workers[12] and Barton and Shirley.[13] This first-order spherical-wave approximation ($SW^{(1)}$) has been shown by Sagurton *et al.*[14] to yield results very close to a rigorous spherical-wave calculation in the case of emission from an s level, but with the advantage of consuming much less computer time. In this work, we apply this $SW^{(1)}$ method for the first time to p-level emission. For this case, there are additional complications due to the occurrence of two different final-state photoelectron channels (s and d) and the resulting interference between the two in all scattering events. As a first attempt to describe our data, we neglect these interference terms and calculate the s- and d-channel scattering independently. Moreover, the d channel is expected to be highly dominant since the ratio of the radial matrix elements R_2/R_0 (before squaring to determine intensities) is about 4.[15] The exact formalism used in these calculations is described in detail elsewhere.[12,14,16]

Figure 2(b) shows the results of d-channel calculations. It is remarkable that most features of the experimental data are quite well reproduced, with the only minor exception being that the intensity rise toward $\theta=40°$, $\phi=45°$, (feature b) that is probably associated with the [111] forward scattering peak is too weak. The regions around the nearest-neighbor emission directions [101] and [011] (features a) are described very well, including the relatively subtle splitting occurring for $\theta \leq 44°$, $\phi=0°,90°$, even though one might expect stronger multiple-scattering effects along these directions.[1,4,9,10] The relative weakness of the ridge b along $\phi=45°$ in our calculations might be due to a slight overestimation of intensity along the nearest-neighbor ⟨110⟩ directions caused by not considering the defocusing aspects of multiple scattering events.[9] However, the degree of agreement found for these ⟨110⟩ directions makes it quite clear that such events do not significantly alter the form or fine structure of the XPD patterns.

With the help of Fig. 2(c), where s-channel calculations are shown, we can also try to assess where interference effects might be strong, although the exact phase relationship between s and d channels has to be known in order to determine whether the intensity will be enhanced or depressed in a certain direction. A proper treatment of these interference terms is currently being implemented in the $SW^{(1)}$ formalism.[16] It is noteworthy that s channel diffraction alone does not agree nearly as well with experiment, e.g., along the ⟨110⟩ directions.

One thing that is evident in Figs. 2(a)–2(c) is that most of the features seem to be sharper and/or more pronounced in the experiment than in theory, particularly for $\theta \gtrsim 45°$. We empirically find that those features can be enhanced in theory by increasing the electron inelastic attenuation length from the 5-Å value used in the calculations (equivalent to 10 Å for wave amplitude attenuation) to 9 Å, which is a suitable literature value for Ni $2p_{3/2}$ photoelectrons at 632 eV.[17] These 9-Å results for the d channel are shown in Fig. 2(d). The value of 5 Å has been used for the calculations in Figs. 2(b) and 2(c) because it yielded best results in plane-wave (PW) and early $SW^{(1)}$ calculations that did not take account of the proper angular momentum of the outgoing photoelectron wave.[10,16] However, while the use of 9 Å clearly improves certain aspects of the features in the center part of the plot ($46° \lesssim \theta \lesssim 50°$, $20° \lesssim \phi \lesssim 70°$), it at the same time seriously deteriorates the rather good correspondence around the ⟨110⟩ directions. This observation may suggest an effective variation of Λ_e with emission direction. One possible reason for this is that along directions with very high charge density such as ⟨110⟩, one expects inelastic events to be more probable than along other, more open higher-index directions. Defocusing multiple-scattering effects along low-index directions[9] could also be a reason. A careful theoretical analysis of the directional dependence of Λ_e in such a crystal is thus of interest.

The question of whether Bragg-like features related to Kikuchi bands can be observed in XPD has been addressed in earlier studies with a much more limited data set.[18] It has been shown that certain XPD patterns in Cu $2p_{3/2}$ emission from Cu(001) exhibit peaks or shoulders at positions that are separated from certain low-index crystal planes by the corresponding Bragg angle θ_B. Also, it has been demonstrated that such features are found in SSC calculations.[18] The data presented in this paper provide a much more detailed test case of this idea, in which the higher angular resolution permits even finer features to be resolved. In Fig. 3 we indicate by solid curves all the positions where first-order Bragg scattering from low-index planes can possibly occur; these are projections of cones that are separated from a given low-index plane by the respective θ_B. The circles indicate positions of peaks (filled circles) and shoulders (open circles) in the experimental scans, seen, e.g., as features d and f in Fig. 1. There is a very close correlation of these data points to certain Bragg positions, thus strongly supporting a Bragg-like origin of these features. Also, the locations of similar features in our SSC calculations (shown as filled and open squares) reproduce experimental data rather well. Also, these theoretical features are all enhanced at higher Λ_e [Fig. 2(d)], as Bragg features should be.[18]

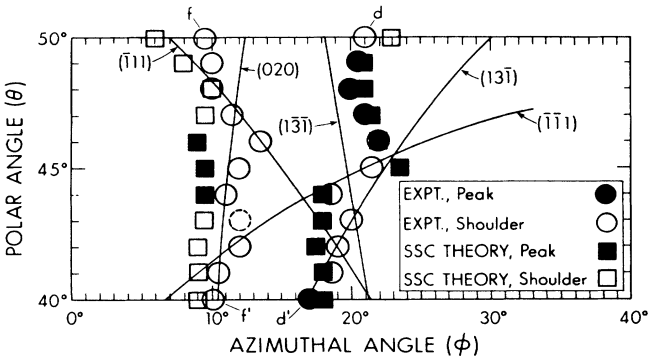

FIG. 3. The positions of all possible first-order Bragg reflections from low-index planes of Ni(001) in Ni $2p_{3/2}$ emission are shown as solid curves. Filled circles correspond to peaks, open circles to shoulders in the experimental data, whereas filled and open squares indicate the positions of corresponding features in our SSC-$SW^{(1)}$ calculations.

Why do we observe certain Bragg events and not others? This is qualitatively explained by noting that the true Bragg condition is never rigorously fulfilled for all waves in XPD because there is always an emitter acting as a point source, rather than a true plane wave source. However, for certain crystal planes and emission directions, the scattered amplitudes can be in phase with one another *and* with the primary, unscattered wave for enough scattering atoms to produce an observable feature at the corresponding Bragg angle.

In conclusion, we find that increased angular resolution in XPD yields intensity patterns with a rich fine structure that should permit more precise structural studies from such data. SSC calculations including spherical-wave corrections for the proper angular-momentum final states reproduce these patterns rather well, including most of the fine structure. Our results thus disagree with a recent assessment[9] of the high importance of multiple scattering in interpreting XPD data. Certain deficiencies in theory, such as an overestimation of intensity along rows of atoms, may be due to a lack of inclusion of proper *s-d* interference, to residual multiple-scattering effects, and/or to a directional dependence of the electron inelastic attenuation. Some of the fine structure in both experiment and theory appears at locations that clearly suggest Bragg-like origin. A more extensive account of this work supports these conclusions and includes azimuthal XPD data from Ni(001) down to $\theta=7°$, as well as calculations with proper *s-d*-channel interference.[16]

This work has been supported by the National Science Foundation under Grant No. CHE83-20200.

[1]S. Kono, S. M. Goldberg, N. F. T. Hall, and C. S. Fadley, Phys. Rev. B **22**, 6085 (1980).

[2]P. J. Orders, S. Kono, C. S. Fadley, R. Trehan, and J. T. Lloyd, Surf. Sci. **119**, 371 (1982).

[3]J. J. Barton, C. C. Bahr, Z. Hussain, S. W. Robey, J. G. Tobin, L. F. Klebanoff, and D. A. Shirley, Phys. Rev. Lett. **51**, 272 (1983); J. J. Barton, S. W. Robey, C. C. Bahr, and D. A. Shirley, in *The Structure of Surfaces,* edited by M. A. van Hove and S. Y. Tong (Springer-Verlag, Berlin, 1985), p. 191.

[4]C. S. Fadley, in *Progress in Surface Science,* edited by S. G. Davison (Pergamon, New York, 1984), Vol. 16, p. 275; Phys. Scr. (to be published).

[5]W. F. Egelhoff, Phys. Rev. B **30**, 1052 (1984).

[6]E. L. Bullock and C. S. Fadley, Phys. Rev. B **31**, 1212 (1984).

[7]K. C. Prince, E. Holub-Krappe, K. Horn, and D. P. Woodruff, Phys. Rev. B **32**, 4249 (1985); D. R. Wesner, F. P. Coenen, and H. P. Bonzel, *ibid.* **33**, 8837 (1986).

[8]J. W. M. Frenken, R. G. Smeenk, and J. F. Van der Veen, Surf. Sci. **135**, 147 (1983).

[9]S. Y. Tong, H. C. Poon, and D. R. Snider, Phys. Rev. B **32**, 2096 (1985).

[10]R. Trehan and C. S. Fadley, Phys. Rev. B **34**, 6784 (1986).

[11]R. C. White, C. S. Fadley, and R. Trehan, J. Electron Spectrosc. Relat. Phenom. **41**, 95 (1986).

[12]J. J. Rehr, R. C. Albers, C. R. Natoli, and E. A. Stern, Phys. Rev. B **34**, 4350 (1986); J. J. Rehr and J. Mustre de Leon (unpublished).

[13]J. J. Barton and D. A. Shirley, Phys. Rev. B **32**, 1892 (1985).

[14]M. Sagurton, E. L. Bullock, R. Saiki, A. Kaduwela, C. R. Brundle, C. S. Fadley, and J. J. Rehr, Phys. Rev. B **33**, 2207 (1986).

[15]S. M. Goldberg, C. S. Fadley, and S. Kono, J. Electron Spectrosc. Relat. Phenom. **21**, 285 (1981).

[16]E. A. Stewart, M. S. thesis, University of Hawaii, 1987 (unpublished); J. Osterwalder, E. A. Stewart, C. S. Fadley, J. Mustre de Leon, and J. J. Rehr (unpublished).

[17]J. Szajman, J. Liesegang, J. G. Jenkin, and R. C. G. Leckey, J. Electron Spectrosc. Relat. Phenom. **23**, 97 (1981).

[18]R. Trehan, J. Osterwalder, and C. S. Fadley, J. Electron Spectrosc. Relat. Phenom. **42**, 187 (1987).